Agreement between a markerless and a marker-based motion capture systems for balance related quantities

Anaïs Chaumeil, Bhrigu Kumar Lahkar, Raphaël Dumas, Antoine Muller, Thomas Robert

Journal Pre-proofs

Agreement between a markerless and a marker-based motion capture systems for balance related quantities

Anaïs Chaumeil, Bhrigu Kumar Lahkar, Raphaël Dumas, Antoine Muller, Thomas Robert

PII: S0021-9290(24)00095-2
DOI: https://doi.org/10.1016/j.jbiomech.2024.112018
Reference: BM 112018

To appear in: *Journal of Biomechanics*

Accepted Date: 19 February 2024

Please cite this article as: A. Chaumeil, B.K. Lahkar, R. Dumas, A. Muller, T. Robert, Agreement between a markerless and a marker-based motion capture systems for balance related quantities, *Journal of Biomechanics* (2024), doi: https://doi.org/10.1016/j.jbiomech.2024.112018

Agreement between a markerless and a marker-based motion capture systems for balance related quantities.

Anaïs Chaumeil[1], Bhrigu Kumar Lahkar[1], Raphaël Dumas[1], Antoine Muller[1], Thomas Robert[1]

[1] Univ Lyon, Univ Eiffel, Univ Claude Bernard Lyon 1, LBMC UMR_T9406, F-69622 Lyon, France

Corresponding author:

raphael.dumas@univ-eiffel.fr

+33 4 72 14 23 56

25 Avenue François Mitterrand

69675 Bron Cedex, France

Keywords: Theia3D; centre of mass; extrapolated centre of mass; angular momentum; markerless vs. marker-based

Word count: 3885 words

Abstract (256 words)

Balance studies usually focus on quantities describing the global body motion. Assessing such quantities using classical marker-based approach can be tedious and modify the participant's behaviour. The recent development of markerless motion capture methods could bypass the issues related to the use of markers. This work compared dynamic balance related quantities obtained with markers and videos. Sixteen young healthy participants performed four different motor tasks: walking at self-selected speed, balance loss, walking on a narrow beam and countermovement jumps. Their movements were recorded simultaneously by marker-based and markerless motion capture systems. Videos were processed using a commercial markerless pose estimation software, Theia3D. The centre of mass position (CoM) was computed, and the associated extrapolated centre of mass position (XCoM) and whole-body angular momentum (WBAM) were derived. Bland-Altman analysis was performed and root mean square difference (RMSD) and coefficient of correlation were computed to compare the results obtained with marker-based and markerless methods. Bias remained of the magnitude of a few mm for CoM and XCoM positions, and RMSD of CoM and XCoM was around 1 cm. RMSD of the WBAM was less than 10% of the total amplitude in any direction, and bias was less than 1%. Results suggest that outcomes of balance studies will be similar whether marker-based or markerless motion capture system are used. Nevertheless, one should be careful when assessing dynamic movements such as jumping, as they displayed the biggest differences (both bias and RMSD), although it is unclear whether these differences are due to errors in markerless or marker-based motion capture system.

Introduction

Balance studies have been conducted to understand the mechanisms that allow humans to maintain their balance in daily life activities such as walking (Silverman and Neptune, 2011), stair climbing (Silverman et al., 2014) or rising from a chair (Fujimoto and Chou, 2012). These studies usually compute a range of biomechanical quantities which allow to describe the dynamic balance of an individual (Bruijn et al., 2013). Whole body linear and angular momenta are widely studied (Bennett et al., 2010; Bruijn et al., 2022; Herr and Popovic, 2008; Kaya et al., 1998) as they characterize the global movement of the body. While studying centre of mass (CoM) position is common in balance studies (Fujimoto and Chou, 2012), another interesting metric proposed by Hof et al. (2005) is the extrapolated centre of mass (XCoM): it is the CoM augmented by a proportion of its own velocity. Its position with respect to the border of the base of support (BoS) is an indicator of the dynamic balance of the participant (Hof et al., 2005). These quantities are of fundamental importance for research in the balance area, and are classically estimated via a segmental approach, using the estimate of the positions, velocities and inertial parameters of the individual body segments.

Classically, dynamic balance related quantities are computed using marker-based motion capture (Buurke et al., 2023; Gill et al., 2019; Silverman et al., 2014). In the absence of easily available ground truth, marker-based motion capture is commonly used, both in research and in clinics (Colyer et al., 2018). Although marker sets have been proposed to reduce the number of markers to be placed on the participant's body (Tisserand et al., 2016), obtaining the segments and whole-body CoM position still requires time and specific marker placement skills. Moreover, the associated experimental constraints limit the validity of the movement studied, as the participants are not in their usual environment, which can cause changes in behaviour (Robles-García et al., 2015).

During the last few years, the field of markerless motion capture systems based on video cameras has drastically expanded (Desmarais et al., 2021). Several aspects of markerless motion analysis have yielded interest in the biomechanics community: ecological validity is enhanced as less strict experimental conditions are required, which allows for data acquisition in a real configuration. It also makes motion analysis more accessible, as it is possible to acquire and process data using low cost hardware such as regular smartphones or webcams and computers (Armitano-Lago et al., 2022). A large number of codes and software are now available, with different approaches and targeted applications (Desmarais et al., 2021; Seethapathi et al., 2019). One of them is Theia3D (Theia Markerless Inc., Kingston, Ontario, Canada), a commercial software designed to study whole-body kinematics with minimal input from the user. Studies have shown that both upper (Lahkar et al., 2022b) and lower (Kanko et al., 2021b; McGuirk et al., 2022) limbs kinematics have a good reliability (Kanko et al., 2021a) and are comparable to those computed using a marker-based system. The same conclusions hold for spatiotemporal gait parameters (McGuirk et al., 2022; Riazati et al., 2022; Kanko et al., 2021c), both in standardized and clinical environment.

Considering the broad emerging literature in markerless motion analysis, few studies have focused on balance related quantities, and, when doing so, the authors mainly consider the CoM position and its derivatives (D'Andrea et al., 2021; Li et al., 2021; Needham et al., 2021a; Tanaka et al., 2019; van den Bogaart et al., 2022; Webering et al., 2021). To the best of our knowledge, Eveleigh et al., (2023) is the only balance study in which Theia3D was used. However, they focused on joint centre position for their analysis and did not compute any of the balance related quantities mentioned prior such as CoM position or whole-body angular momentum (WBAM).

The goal of this study was thus to evaluate, for different motor tasks, the differences of CoM position, XCoM position and WBAM estimated with a markerless pose estimation system, Theia3D, and with a classical marker-based pose estimation system.

Materials and Methods

Experimental session

Sixteen participants (9 men, 7 women) were recruited in this study, with mean age 25.1±3.0 years old, mean body mass index 22.4±3.2 kg/m², mean height 1.7±0.1 m and mean weight 68.4±13.5 kg. Participants had no history of musculoskeletal or balance problems. Prior to the experiment they signed an informed consent form. The study was approved by our institutional review board.

Marker-based optoelectronic and markerless video camera systems were set up for this experiment: 10 Qualisys Miqus M3 cameras recording at 300 Hz and 10 Qualisys Miqus Video recording at 60 Hz (1920 x 1088 pixels). The two systems were synchronized and spatially calibrated using Qualisys Track Manager (QTM – Qualisys AB, Sweden, v2021.1.2). Marker-based and markerless cameras were paired together, and were spaced regularly around the area where the participants performed the movement to capture it fully. For video cameras, auto-exposure mode was selected in QTM and a visual inspection was performed to assess any potential motion blur due to too fast movements and/or too slow shutter speed.

The participants wore minimal, tightly fitting clothing to allow for appropriate marker placement. They were equipped with a full-body marker set comprising 46 markers (Dumas et Wojtusch, 2018; Lahkar et al., 2022a).

The participants performed a static trial (T pose) and four different motor tasks (Figure 1): walking at self-selected speed on a treadmill (**Walk**, between 7 and 20 cycles, corresponding to 10 to 20 seconds, Figure 1A), balance loss (**Lean**, lean forward until loss of balance requiring

one or more recovery steps, 3 repetitions, Figure 1B), walking on a 2 m long, 2.3 cm wide and 5 cm high beam (**Beam**, 4 repetitions of walking the full length of the beam, Figure 1C) and countermovement jumps (**CMJS**, 3 repetitions, Figure 1D). Tasks were explained and shown to the participants, and they could train before the recording of each task. Walking speed was determined by increasing treadmill speed starting from 0.1m/s to a participant-selected comfortable speed by 0.05m/s increments. These tasks were chosen as they were representative of different speeds (slow, normal, fast) and occurred in different planes of movement (sagittal and frontal planes). Beginning and end of the tasks were defined manually during the post-processing phase, with a margin of approximately 1s before and after the movement.

[INSERT FIGURE 1]

Data processing

Markerless data

Markerless data was processed with Theia3D, a deep learning-based commercial software, with both versions v2021.2 and v2023.1.0.3160. Results presented in this paper were obtained using v2023.1.0.3160. Results for v2021.2 can be found in Supplementary Materials S2. It uses deep learning techniques and inverse kinematics (IK) to estimate 3D pose of a subject of interest based on multi-camera video data and the associated calibration file (Kanko et al., 2021b). The outputs of Theia3D were composed of a 17-segment kinematic model defined independently in Theia3D for each trial with 56 degrees of freedom (DoFs) (segments: head, thorax, upper arms, forearms, hands, pelvis, thighs, shanks, feet and toes; joints: free joints (6 DoFs) for the head, pelvis and thorax, shoulders (5 DoFs), elbows (2 DoFs), wrists (2 DoFs), hips (3 DoFs), knees (3 DoFs), ankles (3 DoFs), metatarsophalangeal joint (1 DoF)) and the non-filtered pose matrices associated with each segment. These outputs were exported in Visual3D (C-motion, Germantown, USA, v2021.11.3) and body segment inertial parameters (BSIPs – segment mass,

position of segment CoM and moment of inertia) were added to the kinematic model according to Dumas et Wojtusch (2018). The markerless model was described in more details in Lahkar et al., (2022a).

Marker-based data

Marker-based data was first processed in QTM, including labelling and either linear or relational gap filling of marker trajectories. No frame was excluded because of missing marker after QTM processing. Then, labelled and cleaned marker positions were imported in Visual3D where custom models were created for each participant using the static trial. IK was finally performed using a multibody kinematics optimization (Lu and O'Connor, 1999). The marker-based kinematic model was built based on Dumas et Wojtusch (2018). The model was composed of 17 segments and 54 DoFs (segments: head, thorax, clavicles, upper arms, forearms, hands, pelvis, thighs, shanks, feet; joints: free joints (6 DoFs) for the head, pelvis and thorax, shoulders (5 DoFs), elbows (2 DoFs), wrists (2 DoFs), hips (3 DoFs), knees (3 DoFs),

ankles (3 DoFs)). More information about the marker-based model can be found in Lahkar et al., (2022a).

Computing balance related quantities

For both marker-based and markerless data, the following quantities were exported frame-by-frame from Visual3D following the IK step:

- the position of the CoM for each segment and the whole body;
- the linear velocity of the CoM of each segment;
- the angular velocity of each segment;
- the rotation matrix associated with each segment.

Using MATLAB (MathWorks, USA), the positions and velocities of segments' CoM and their angular velocities were filtered using a 4th order Butterworth filter with a 7 Hz cut-off frequency (Winter, 2009). The velocity of the global CoM was obtained by differentiating the CoM and filtering the resulting signal with the same parameters. XCoM position was computed based on Hof et al., (2005) as:

$$\overrightarrow{XCOM} = \overrightarrow{COM} + \frac{\overrightarrow{v_{com}}}{\omega_0} \qquad (1)$$

where $\overrightarrow{COM}$ is the vector representing the position of the whole-body's CoM with respect to the laboratory reference frame origin, $\overrightarrow{v_{com}}$ its velocity and $\omega_0 = \sqrt{g/l}$ is a constant with $g = 9.81 m/s^2$ and l the height of the CoM of the participant, approximated as half of their declared height.

WBAM about the CoM was computed as:

$$\overrightarrow{WBAM} = \sum_{i=1}^{n} \left[\left(\overrightarrow{COM_i} - \overrightarrow{COM} \right) \times m_i (\overrightarrow{v_{comi}} - \overrightarrow{v_{com}}) \right] + I_i * \overrightarrow{\omega_i} \qquad (2)$$

$\overrightarrow{COM}$ and $\overrightarrow{v_{com}}$ are respectively the position and velocity of the global CoM, $\overrightarrow{COM_i}$ and $\overrightarrow{v_{com_i}}$ are respectively the position and velocity of the i^{th} segment's CoM, m_i is its mass, I_i its inertial matrix expressed in the laboratory reference frame (computed using the inertias about the segment axes and the rotation matrix) and $\overrightarrow{\omega_i}$ the angular velocity of the i^{th} segment with respect to the laboratory.

$WBAM$ was made unitless as in (Begue et al., 2021) by dividing it by $m\sqrt{g/h}$, with h being the height of the participant and m it's mass.

Both marker-based and markerless-based data were computed across all the available frames, and marker-based CoM position, XCoM position and WBAM were finally down-sampled at 60Hz to match markerless-based data frequency.

Statistical analysis

The level of similarity between marker-based and markerless results was assessed by computing Bland Alman (Bland and Altman, 1986) bias and limits of agreement (LOA). Differences between markerless and marker-based results (markerless - marker-based) were plotted against their mean. Root mean square difference (RMSD) and Pearson coefficient of correlation (R^2) were also computed. Bias, LOA and R^2 were computed using an available MATLAB toolbox (Klein, 2023). The quantities of interest were CoM position, XCoM position and WBAM, the latter being expressed both as a unitless value and as a percentage of the amplitude (computed as ±3 standard deviations across all motor tasks and averaged over markerless and marker-based data). All the statistical parameters were computed across all tasks and for each task separately, for all subjects.

Results

All trials but three (one **Beam** and two **CMJS**) could be fully processed. Table 1 displays the statistical parameters bias, LOA, RMSD and R^2 for the WBAM (expressed both as unitless and as a percentage of the total amplitude), CoM and XCoM positions, computed across all tasks and for each task separately. Three directions were considered here: anterior-posterior (AP), medial-lateral (ML) and superior-inferior (SI). Spreadsheets containing the statistical parameters for both v2023.1.0.3160 and v2021.2 were placed in Supplementary Materials S2. Minimal differences were observed between the results of the two versions, and thus only the results of v2023 were presented here. Bland Altman plots for unitless WBAM, CoM and XCoM position can be found in Supplementary Materials (Figure S1).

CoM

The bias of CoM position (markerless - marker-based) ranged from few tenth of mm in AP and ML directions (respectively 0.025 cm and 0.061 cm across all tasks) to around 1 cm in SI direction (-1.17 cm across all tasks). In SI direction, bias was negative for all tasks. The LOA remained smaller than 2 cm for all tasks, being under 1 cm for all tasks in ML direction and above 1 cm for all tasks in AP and SI directions. RMSD remained under 1 cm except in SI direction for all movements, being smaller in ML direction for all tasks (Figure 2 A). The coefficients of correlation were substantial (0.98 to 0.99).

XCoM

The bias of XCoM position displayed results similar to the bias of CoM position: it was negative and around 1 cm in the SI direction (-1.14 cm across all tasks), and equal to a few mm in AP and ML directions (respectively 0.026 cm and 0.061 cm across all tasks). The LOA remained smaller than 2 cm except for **CMJS** in the SI direction (2.83 cm). For both LOA and RMSD, the values were always smaller in the ML direction regardless of the task. RMSD ranged from few mm to 2 cm. RMSD was systematically higher than 1 cm for all tasks in the SI direction,

and it was higher than 2 cm for the **CMJS** movement (2.09 cm). The coefficients of determination were substantial (0.97 to 0.99).

WBAM

The order of magnitude of the RMSD of the unitless WBAM across all tasks was the same in all three directions (Figure 2, C), although it did not represent the same percentage of the amplitude (Figure 2, D): the RMSD in the SI direction represented 7.58% of the amplitude of the WBAM, while it was less than 4% in the AP (3.16%) and ML (3.87%) directions. This trend was similar for each task and can also be noticed for the LOA. The RMSD expressed in percentage of the amplitude was bigger in the SI direction: the unitless RMSD was of the same order of magnitude as for AP and ML directions but was divided by a smaller amplitude (0.0279, 0.0239 and 0.0090 in AP, ML and SI directions respectively). It thus led to bigger percentages (Figure 2, C & D). Regarding R^2, it ranged from moderate (0.63) to substantial (0.99), with the **CMJS** being the task with the smallest R^2 in SI (0.63) and AP (0.65) directions.

[INSERT FIGURE 2]

[INSERT TABLE 1]

Discussion

This study aimed at assessing commonly used quantities in balance studies, CoM position, XCoM position and WBAM, estimated with a markerless pose estimation software, Theia3D, and comparing the results to the estimation obtained with a marker-based method. Overall, the values of RMSD between the two measurement systems were around 1 cm for the CoM and XCoM positions and less than 10% of the amplitude for the WBAM.

The RMSD obtained when comparing CoM position computed with the markerless and marker-based systems had a magnitude of around 1 cm, and the associated LOA remained under 2 cm across all tasks, suggesting a minimal dispersion of the results. Few studies have compared CoM position computed using these two approaches. Needham et al., (2021a) focused on computing CoM position during sprinting, using an open source markerless software and a full body marker set. Mean difference of CoM position between the two measurement methods was between 1 mm and 9 mm, depending on the applied filter during post processing. They also provided standard deviations which ranged from 16 mm to 32 mm. The RMSD and LOA values obtained in our study for CoM position across all tasks (from 3.3 mm to 12.9 mm for the RMSD and from 5.5 mm to 15.4 mm for the LOA) were consistent with those obtained by Needham et al., (2021a).

The RMSD and LOA obtained for XCoM position had the same order of magnitude as the ones obtained for CoM position, which was consistent as the XCoM was computed based on CoM. In the literature, the simplified marker set proposed by Tisserand et al., (2016) has been used to compute XCoM position during gait and fall recovery, and the resulting XCoM position was compared to the XCoM position obtained using the marker set of Dumas et al., (2007). Mean difference between XCoM position computed using simplified and reference models ranged from 7.8±3.4 mm to 8.5±2.8 mm. This reported magnitude of difference of XCoM position computed using the reference and simplified models was similar to that obtained in our study (from 4.7 mm to 14.7 mm). As the simplified marker set was adopted in other studies, this magnitude of difference seems acceptable. To the best of our knowledge, no study has been conducted to compare XCoM position computed with markerless and marker-based approaches. It is however questionable whether such differences are acceptable when comparing groups with different conditions, especially in the clinical context. In their repeatability study, de Jong et al (2020) have computed distances between XCoM position,

measured with markers, and the centre of pressure (CoP), measured reliably with an instrumented treadmill, during gait. During one of their measurement sessions, they found differences of approximately 300 mm in the AP direction and 25 mm in the ML direction between the control and patient groups. These differences were higher than the differences of XCoM positions observed between markerless and marker-based systems. However, when comparing the stroke patients and spinal cord injury patient groups (de Jong et al., 2020), the differences dropped to approximately 70 mm and 4 mm in the AP and ML directions respectively. It should thus be verified beforehand if the accuracy required for the clinical application is compatible with the differences (bias and LOA) that can be found between markerless and marker-based systems.

It was more difficult to compare the results we obtained for the WBAM to the literature because of the different existing normalizations techniques. Begue et al. (2021) have studied WBAM, expressed with the same normalization, for young and old adults during stepping at preferred and fast speeds. The smallest significant difference they found was of $0.6 \cdot 10^{-3}$ (unitless). It was the same order of magnitude as the RMSD found in our study for the WBAM across all tasks ($0.51 \cdot 10^{-3}$ to $0.60 \cdot 10^{-3}$, unitless). The other differences found in their study were bigger (from $1.6 \cdot 10^{-3}$ to $5.9 \cdot 10^{-3}$ unitless) and were outside of the LOA we found (between $0.68 \cdot 10^{-3}$ and $0.93 \cdot 10^{-3}$ unitless). It seemed therefore also possible to use a markerless system to compute WBAM and compare groups and conditions in balance studies, but one should be aware of the order of magnitude of the differences found between the conditions, as the differences could be partly due to using the markerless instead of marker-based motion capture system.

Absolute value of the bias is systematically higher in SI direction for CoM position across all tasks, being above 1 cm for all tasks except **CMJS** (0.78 cm). Bias in this direction is also negative, indicating that CoM position computed with markerless data is systematically below CoM position computed with marker-based data. This could be due to model differences, as the

markerless and marker-based models were built using different approaches (Lahkar et al., 2022a). Indeed, limited information was available regarding the markerless model and it was not possible to modify segment definition. For the markerless model, the inverse kinematics process was run directly in Theia3D and it was not possible to modify the model at this level, thus only the BSIPs could be added to match an anthropometric table (Dumas et Wojtusch, 2018) in Visual3D. The marker-based model was also built based on (Dumas et Wojtusch, 2018), but no adaptation were made to specifically match the markerless model segment definition. In Lahkar et al., (2022a), CoM position for each segment and for the whole-body in the static position between markerless and marker-based models were compared in the global coordinate system. For whole-body CoM position, mean differences between - 0.1±2.5 mm and - 2.8±7.0 mm were found. Differences could be bigger for each individual segment, with differences as high as 27.3±8.8 mm for the thigh in AP direction and - 8.5±4.9 mm for the right forearm in SI direction for example. These observed differences highlight the differences between markerless and marker-based model construction in a static position.

It appears that the task performed and the associated dynamic aspect have an influence on the differences obtained between the two measurement systems, which is consistent with the findings of previous studies (Nakano et al., 2020; Needham et al., 2021b). For CoM and XCoM positions in SI direction, bias and RMSD had similar values with only a few millimetres of difference for all tasks except **CMJS**. It suggests that when the dynamic aspect of the task was limited (i.e., for **Walk**, **Lean** and **Beam**), most of the RMSD in the SI direction could be explained by the bias, which was likely due to model differences. However, when the task was more dynamic, such as **CMJS**, part of the RMSD could be explained by the larger marker movement, especially with soft tissue artefacts. Moreover, the difference of RMSD between the main direction of movement (SI) and the two other directions was higher for XCoM position than for CoM position for **CMJS**, as the XCoM included the velocity of the CoM in its

expression (Figure 2 A & B). Moreover, for all the tasks, the smallest RMSD of the CoM and XCoM positions is systematically in the ML direction: as these tasks take place in the sagittal plane, there is little displacement and small velocity in the ML direction, thus the difference of measurement is reduced. There is no similar phenomenon for WBAM, as no direction displayed a systematically higher bias or RMSD. Despite the observations noted above regarding the dynamic aspect of the tasks, it should still be noted that the differences remained of the magnitude of the centimetre.

There are some limitations to this study. First, participants were healthy young adults, and it is a possibility that the dataset used to train the neural network of the markerless system contained mainly similar subjects. It is thus relevant to wonder if the same results would be obtained with participants with different ages and/or anthropometric characteristics, or patients with body deformities. Moreover, this study was conducted in a controlled laboratory environment: participants were wearing minimally fitting clothes, the lightning conditions were controlled and there was a consequent number of cameras. All these parameters are currently under study in the literature to understand their effect on the accuracy of markerless motion capture (Keller et al., 2022; Pagnon et al., 2021; Viswakumar et al., 2019). Markers were also clearly visible in the videos. To the best of our knowledge, no study has evaluated the effect of the presence or absence of markers in video for deep learning identification of landmarks. However, some studies have evaluated the effect of the clothing conditions (Keller et al., 2022) and found no meaningful changes in the estimated parameters (segment lengths, spatiotemporal gait parameters, …). It is thus likely that the presence or absence of markers would also have limited impact on landmark estimation. Another limitation is that markerless data was compared to marker-based data, which itself can be prone to errors due to marker placement and soft tissue artefacts. However, in the absence of a ground truth measurement, it was not possible to associate the differences obtained in this study to one measurement system or another.

Conclusion

In this study, we assessed whether a markerless motion capture system, Theia3D, can be used to compute quantities that are widely used in balance-related studies. The results showed a moderate to substantial level of agreement between the markerless and marker-based systems. With such differences, a markerless approach thus seems a reasonable alternative to marker-based systems for balance studies.

Acknowledgment

This study was supported by the ANR grant 20-STHP-0003.

Conflicts of interest

The authors declare that they have no financial or personal relationships that could inappropriately influence their work.

References

Armitano-Lago, C., Willoughby, D., Kiefer, A.W., 2022. A SWOT Analysis of Portable and Low-Cost Markerless Motion Capture Systems to Assess Lower-Limb Musculoskeletal Kinematics in Sport. Front. Sports Act. Living 3, 809898. https://doi.org/10.3389/fspor.2021.809898

Begue, J., Peyrot, N., Lesport, A., Turpin, N.A., Watier, B., Dalleau, G., Caderby, T., 2021. Segmental contribution to whole-body angular momentum during stepping in healthy young and old adults. Sci. Rep. 11, 19969. https://doi.org/10.1038/s41598-021-99519-y

Bennett, B.C., Russell, S.D., Sheth, P., Abel, M.F., 2010. Angular momentum of walking at different speeds. Hum. Mov. Sci. 29, 114–124. https://doi.org/10.1016/j.humov.2009.07.011

Bland, J.M., Altman, D.G., 1986. Statistical methods for assessing agreement between two methods of clinical measurement. Lancet Lond. Engl. 1, 307–310.

Bruijn, S.M., Meijer, O.G., Beek, P.J., van Dieën, J.H., 2013. Assessing the stability of human locomotion: a review of current measures. J. R. Soc. Interface 10, 20120999. https://doi.org/10.1098/rsif.2012.0999

Bruijn, S.M., Sloot, L.H., Kingma, I., Pijnappels, M., 2022. Contribution of arm movements to balance recovery after tripping in older adults. J. Biomech. 133, 110981. https://doi.org/10.1016/j.jbiomech.2022.110981

Buurke, T.J.W., van de Venis, L., den Otter, R., Nonnekes, J., Keijsers, N., 2023. Comparison of ground reaction force and marker-based methods to estimate mediolateral center of mass displacement and margins of stability during walking. J. Biomech. 146, 111415. https://doi.org/10.1016/j.jbiomech.2022.111415

Colyer, S.L., Evans, M., Cosker, D.P., Salo, A.I.T., 2018. A Review of the Evolution of Vision-Based Motion Analysis and the Integration of Advanced Computer Vision Methods Towards Developing a Markerless System. Sports Med. - Open 4, 24. https://doi.org/10.1186/s40798-018-0139-y

D'Andrea, D., Cucinotta, F., Farroni, F., Risitano, G., Santonocito, D., Scappaticci, L., 2021. Development of Machine Learning Algorithms for the Determination of the Centre of Mass. Symmetry 13, 401. https://doi.org/10.3390/sym13030401

de Jong, L.A.F., van Dijsseldonk, R.B., Keijsers, N.L.W., Groen, B.E., 2020. Test-retest reliability of stability outcome measures during treadmill walking in patients with balance problems and healthy controls. Gait Posture 76, 92–97. https://doi.org/10.1016/j.gaitpost.2019.10.033

Desmarais, Y., Mottet, D., Slangen, P., Montesinos, P., 2021. A review of 3D human pose estimation algorithms for markerless motion capture. ArXiv201006449 Cs.

Dumas, R., Chèze, L., Verriest, J.-P., 2007. Adjustments to McConville et al. and Young et al. body segment inertial parameters. J. Biomech. 40, 543–553. https://doi.org/10.1016/j.jbiomech.2006.02.013

Dumas, R., Wojtusch, J., 2018. Estimation of the Body Segment Inertial Parameters for the Rigid Body Biomechanical Models Used in Motion Analysis, in: Handbook of Human Motion. Springer International Publishing, Cham, pp. 47–77. https://doi.org/10.1007/978-3-319-14418-4_147

Eveleigh, K.J., Deluzio, K.J., Scott, S.H., Laende, E.K., 2023. Principal component analysis of whole-body kinematics using markerless motion capture during static balance tasks. J. Biomech. 152, 111556. https://doi.org/10.1016/j.jbiomech.2023.111556

Fujimoto, M., Chou, L.-S., 2012. Dynamic balance control during sit-to-stand movement: An examination with the center of mass acceleration. J. Biomech. 45, 543–548. https://doi.org/10.1016/j.jbiomech.2011.11.037

Gill, L., Huntley, A.H., Mansfield, A., 2019. Does the margin of stability measure predict medio-lateral stability of gait with a constrained-width base of support? J. Biomech. 95, 109317. https://doi.org/10.1016/j.jbiomech.2019.109317

Herr, H., Popovic, M., 2008. Angular momentum in human walking. J. Exp. Biol. 211, 467–481. https://doi.org/10.1242/jeb.008573

Hof, A.L., Gazendam, M.G.J., Sinke, W.E., 2005. The condition for dynamic stability. J. Biomech. 38, 1–8. https://doi.org/10.1016/j.jbiomech.2004.03.025

Kanko, R.M., Laende, E., Selbie, W.S., Deluzio, K.J., 2021a. Inter-session repeatability of markerless motion capture gait kinematics. J. Biomech. 121, 110422. https://doi.org/10.1016/j.jbiomech.2021.110422

Kanko, R.M., Laende, E.K., Davis, E.M., Selbie, W.S., Deluzio, K.J., 2021b. Concurrent assessment of gait kinematics using marker-based and markerless motion capture. J. Biomech. 127, 110665. https://doi.org/10.1016/j.jbiomech.2021.110665

Kanko, R.M., Strutzenberger, G., Brown, M., Selbie, S., Deluzio, K., 2021c. Assessment of spatiotemporal gait parameters using a deep learning algorithm-based markerless motion capture system 17.

Kaya, B.K., Krebs, D.E., Riley, P.O., 1998. Dynamic Stability in Elders: Momentum Control in Locomotor ADL. J. Gerontol. A. Biol. Sci. Med. Sci. 53A, M126–M134. https://doi.org/10.1093/gerona/53A.2.M126

Keller, V.T., Outerleys, J.B., Kanko, R.M., Laende, E.K., Deluzio, K.J., 2022. Clothing condition does not affect meaningful clinical interpretation in markerless motion capture. J. Biomech. 141, 111182. https://doi.org/10.1016/j.jbiomech.2022.111182

Klein, R., 2023. Bland-Altman and Correlation Plot [WWW Document]. MATLAB Cent. File Exch. URL https://www.mathworks.com/matlabcentral/fileexchange/45049-bland-altman-and-correlation-plot (accessed 11.24.23).

Lahkar, B.K., Chaumeil, A., Dumas, R., Muller, A., Robert, T., 2022a. Description, Development and Dissemination of Two Consistent Marker-based and Markerless Multibody Models (preprint). Bioengineering. https://doi.org/10.1101/2022.11.08.515577

Lahkar, B.K., Muller, A., Dumas, R., Reveret, L., Robert, T., 2022b. Accuracy of a markerless motion capture system in estimating upper extremity kinematics during boxing. Front. Sports Act. Living 11. https://doi.org/doi: 10.3389/fspor.2022.939980

Li, B., Williamson, J., Kelp, N., Dick, T., Bo, A.P.L., 2021. Towards balance assessment using Openpose, in: 2021 43rd Annual International Conference of the IEEE Engineering in Medicine & Biology Society (EMBC). Presented at the 2021 43rd Annual International Conference of the IEEE Engineering in Medicine & Biology Society (EMBC), IEEE, Mexico, pp. 7605–7608. https://doi.org/10.1109/EMBC46164.2021.9631001

Lu, T.-W., O'Connor, J.J., 1999. Bone position estimation from skin marker co-ordinates using global optimisation with joint constraints. J. Biomech. 32, 129–134. https://doi.org/10.1016/S0021-9290(98)00158-4

McGuirk, T.E., Perry, E.S., Sihanath, W.B., Riazati, S., Patten, C., 2022. Feasibility of Markerless Motion Capture for Three-Dimensional Gait Assessment in Community Settings. Front. Hum. Neurosci. 16.

Nakano, N., Sakura, T., Ueda, K., Omura, L., Kimura, A., Iino, Y., Fukashiro, S., Yoshioka, S., 2020. Evaluation of 3D Markerless Motion Capture Accuracy Using OpenPose With Multiple Video Cameras. Front. Sports Act. Living 2, 50. https://doi.org/10.3389/fspor.2020.00050

Needham, L., Evans, M., Cosker, D.P., Colyer, S.L., 2021a. Can Markerless Pose Estimation Algorithms Estimate 3D Mass Centre Positions and Velocities during Linear Sprinting Activities? Sensors 21, 2889. https://doi.org/10.3390/s21082889

Needham, L., Evans, M., Cosker, D.P., Wade, L., McGuigan, P.M., Bilzon, J.L., Colyer, S.L., 2021b. The accuracy of several pose estimation methods for 3D joint centre localisation. Sci. Rep. 11, 20673. https://doi.org/10.1038/s41598-021-00212-x

Pagnon, D., Domalain, M., Reveret, L., 2021. Pose2Sim: An End-to-End Workflow for 3D Markerless Sports Kinematics—Part 1: Robustness. Sensors 21, 6530. https://doi.org/10.3390/s21196530

Riazati, S., McGuirk, T.E., Perry, E.S., Sihanath, W.B., Patten, C., 2022. Absolute Reliability of Gait Parameters Acquired With Markerless Motion Capture in Living Domains. Front. Hum. Neurosci. 16.

Robles-García, V., Corral-Bergantiños, Y., Espinosa, N., Jácome, M.A., García-Sancho, C., Cudeiro, J., Arias, P., 2015. Spatiotemporal Gait Patterns During Overt and Covert Evaluation in Patients With Parkinson's Disease and Healthy Subjects: Is There a Hawthorne Effect? J. Appl. Biomech. 31, 189–194. https://doi.org/10.1123/jab.2013-0319

Seethapathi, N., Wang, S., Saluja, R., Blohm, G., Kording, K.P., 2019. Movement science needs different pose tracking algorithms. ArXiv190710226 Cs Q-Bio.

Silverman, A.K., Neptune, R.R., 2011. Differences in whole-body angular momentum between below-knee amputees and non-amputees across walking speeds. J. Biomech. 44, 379–385. https://doi.org/10.1016/j.jbiomech.2010.10.027

Silverman, A.K., Neptune, R.R., Sinitski, E.H., Wilken, J.M., 2014. Whole-body angular momentum during stair ascent and descent. Gait Posture 39, 1109–1114. https://doi.org/10.1016/j.gaitpost.2014.01.025

Tanaka, R., Ishii, Y., Yamasaki, T., Kawanishi, H., 2019. Measurement of the total body center of gravity during sit-to-stand motion using a markerless motion capture system. Med. Eng. Phys. 66, 91–95. https://doi.org/10.1016/j.medengphy.2018.12.020

Theia Markerless - Markerless Motion Capture Redefined [WWW Document], n.d. . Theia Markerless. URL https://www.theiamarkerless.ca/ (accessed 7.18.22).

Tisserand, R., Robert, T., Dumas, R., Chèze, L., 2016. A simplified marker set to define the center of mass for stability analysis in dynamic situations. Gait Posture 48, 64–67. https://doi.org/10.1016/j.gaitpost.2016.04.032

van den Bogaart, M., Bruijn, S.M., Spildooren, J., van Dieën, J.H., Meyns, P., 2022. Effects of age and surface instability on the control of the center of mass. Hum. Mov. Sci. 82, 102930. https://doi.org/10.1016/j.humov.2022.102930

Viswakumar, A., Rajagopalan, V., Ray, T., Parimi, C., 2019. Human Gait Analysis Using OpenPose, in: 2019 Fifth International Conference on Image Information Processing (ICIIP). Presented at the 2019 Fifth International Conference on Image Information Processing (ICIIP), IEEE, Shimla, India, pp. 310–314. https://doi.org/10.1109/ICIIP47207.2019.8985781

Webering, F., Blume, H., Allaham, I., 2021. Markerless camera-based vertical jump height measurement using OpenPose, in: 2021 IEEE/CVF Conference on Computer Vision and Pattern Recognition Workshops (CVPRW). Presented at the 2021 IEEE/CVF Conference on Computer Vision and Pattern Recognition Workshops (CVPRW), IEEE, Nashville, TN, USA, pp. 3863–3869. https://doi.org/10.1109/CVPRW53098.2021.00428

Winter, D.A., 2009. Biomechanics and motor control of human movement, 4th ed. ed. Wiley, Hoboken, N.J.

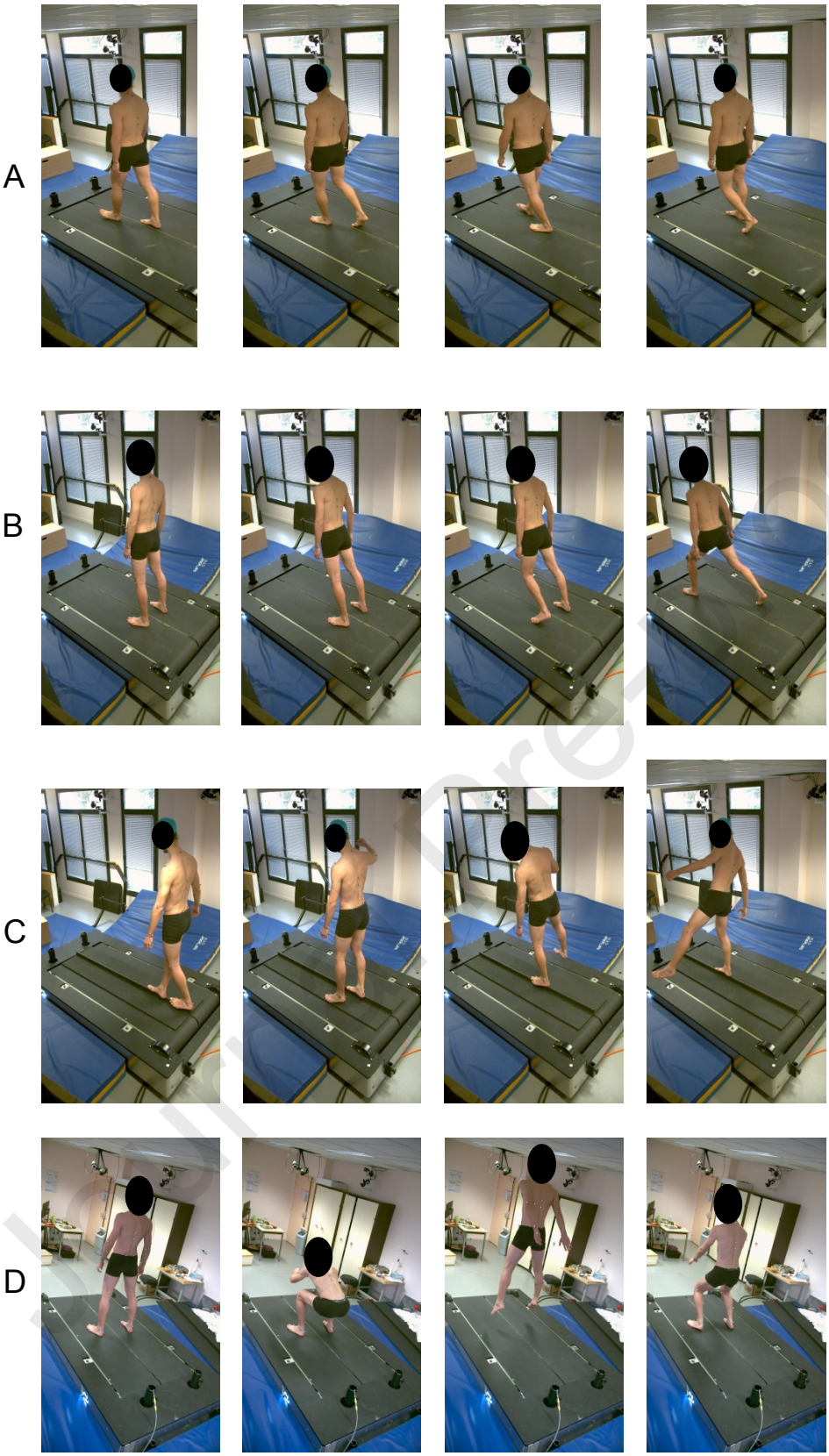

Figure 1: Snapshots of the tasks performed during the experimental session by a participant. A: Walk, B: Lean, C: Beam, D: CMJS.

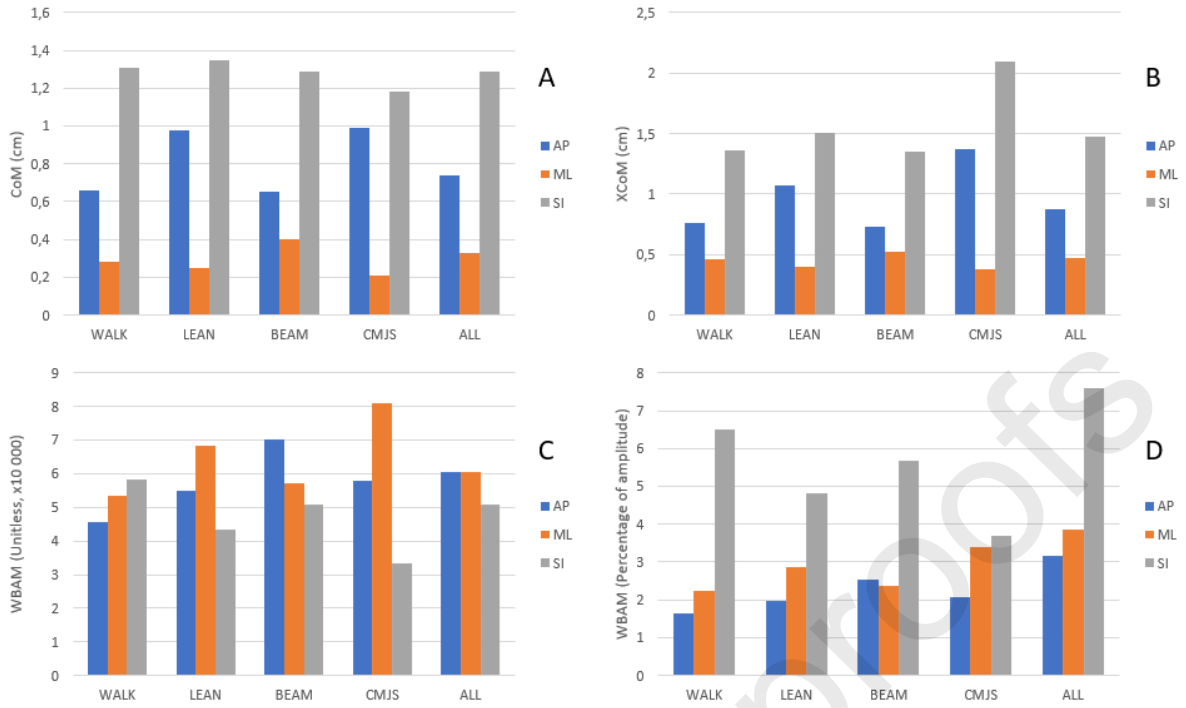

Figure 2: RMSD of the CoM in cm (A), XCoM in cm (B), unitless WBAM (C) and WBAM expressed as a percentage of the amplitude (D), for each task and across all tasks in the AP (blue), ML (orange) and SI (grey) directions. (For interpretation of the references to color in this figure legend, the reader is referred to the web version of this article.)

Table 1: Results of the Bland-Altman analysis for each task and across all tasks, for all participants. For unitless WBAM, values have been multiplied by 10 000 (except R^2) and displayed for easier reading. Bias is computed as markerless minus marker-based data. Across all tasks, more than 54 000 frames were considered.

		Walk			Lean			Beam			CMJS			All tasks		
		AP	**ML**	**SI**	**AP**	**ML**	**SI**	**AP**	**ML**	**SI**	**AP**	**ML**	**SI**	**AP**	**ML**	**SI**
CoM (cm)	**Bias**	0.19	0.10	-1.29	0.68	0.061	-1.27	0.14	0.10	-1.20	0.57	-0.037	-0.78	0.025	0.061	-1.17
	LOA	1.24	0.54	1.81	1.35	0.49	1.64	1.39	0.69	1.08	1.39	0.39	1.61	1.40	0.58	1.54
	RMSD	0.66	0.28	1.31	0.98	0.25	1.35	0.65	0.40	1.29	0.99	0.21	1.18	0.74	0.33	1.29
	R^2	0.99	0.99	0.98	0.99	0.99	0.98	0.99	0.99	0.99	0.99	0.99	0.99	0.99	0.99	0.99
XCoM (cm)	**Bias**	0.21	0.095	-1.07	0.67	-0.041	-1.25	0.13	0.11	-1.19	0.57	-0.023	-0.74	0.026	0.061	-1.14
	LOA	1.32	0.86	1.97	1.47	0.60	1.76	1.42	0.87	1.34	1.99	0.63	2.83	1.50	0.80	1.71
	RMSD	0.76	0.46	1.36	1.07	0.40	1.51	0.73	0.52	1.35	1.37	0.38	2.09	0.88	0.47	1.47
	R^2	0.99	0.99	0.98	0.99	0.99	0.98	0.99	0.99	0.98	0.99	0.98	0.99	0.99	0.99	0.99
WBAM (unitless, x E-04 except R^2)	**Bias**	0.13	0.43	0.15	0.16	0.72	-0.12	0.046	-0.015	0.10	0.60	0.47	-0.023	0.15	0.28	0.034
	LOA	8.88	10.16	8.96	3.31	6.37	2.79	10.34	8.68	7.28	9.83	14	0.539	8.81	9.27	6.80
	RMSD	4.55	5.33	5.83	5.49	6.85	4.33	7.02	5.71	5.10	5.79	8.09	3.32	6.06	6.05	5.08
	R^2	0.94	0.96	0.72	0.93	0.98	0.87	0.99	0.98	0.93	0.65	0.97	0.63	0.99	0.98	0.89
WBAM (% of amplitude)	**Bias**	0.046	0.18	0.17	0.058	0.30	-0.14	0.016	-0.0066	0.11	0.21	0.20	-0.026	0.052	0.11	0.038
	LOA	3.18	4.25	9.99	1.19	2.66	3.12	3.71	3.63	8.12	3.53	5.71	6.01	2.17	2.53	5.67
	RMSD	1.63	2.23	6.51	1.97	2.86	4.83	2.52	2.38	5.69	2.07	3.38	3.70	3.16	3.87	7.58
	R^2	0.94	0.96	0.72	0.93	0.98	0.87	0.99	0.98	0.93	0.65	0.97	0.63	0.99	0.98	0.89

Supplementary materials

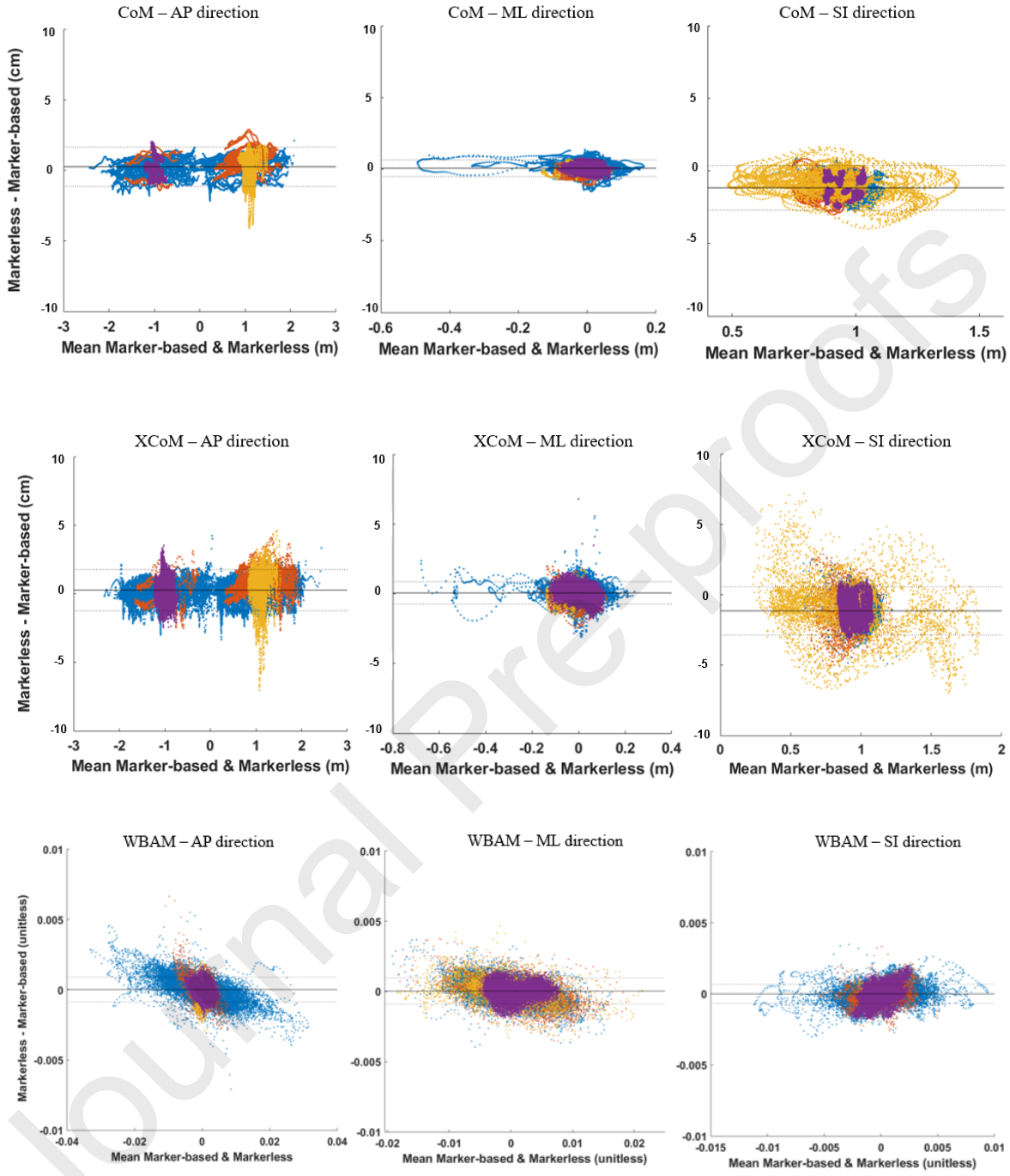

Figure S1: Bland Altman plots. Each line corresponds to one of the measured quantities (top to bottom: CoM, XCoM, WBAM) and each column corresponds to one direction (left to right: AP, ML, SI). Each point represents one frame, all participants are included. Each color represents one task: **Walk** is in purple, **Lean** is in orange, **Beam** is in blue and **CMJS** is in yellow. It should be noted that, for CoM and XCoM, the abscissa has little interest for our study: it represents the position of the participant in the laboratory reference frame. Solid horizontal line represents the bias, and dotted lines represent the limits of agreement.

Conflict of interest

The authors have no financial or personal relationships with other people or organizations that could have inappropriately influenced their work.